13. Bergman AM, Eijk PP, Ruiz van Haperen VW, Smid K, Veerman G, Hubeek I, van den Ijssel P, Ylstra B, Peters GJ. In vivo induction of resistance to gemcitabine results in increased expression of ribonucleotide reductase subunit M1 as the major determinant. Cancer Res 2005;65:9510–16.
14. Dumontet C, Bauchu EC, Fabianowska K, Lepoivre M, Wyczechowska D, Bodin F, Rolland MO. Common resistance mechanisms to nucleoside analogues in variants of the human erythroleukemic line K562. Adv Exp Med Biol 1999;457:571–7.
15. Duxbury MS, Ito H, Zinner MJ, Ashley SW, Whang EE. RNA interference targeting the M2 subunit of ribonucleotide reductase enhances pancreatic adenocarcinoma chemosensitivity to gemcitabine. Oncogene 2004;23:1539–48.
16. Galmarini CM, Clarke ML, Jordheim L, Santos CL, Cros E, Mackey JR, Dumontet C. Resistance to gemcitabine in a human follicular lymphoma cell line is due to partial deletion of the deoxycytidine kinase gene. BMC Pharmacol 2004;4:8.
17. Eliopoulos N, Cournoyer D, Momparler RL. Drug resistance to 5-aza-2′-deoxycytidine, 2′,2′-difluorodeoxycytidine, and cytosine arabinoside conferred by retroviral-mediated transfer of human cytidine deaminase cDNA into murine cells. Cancer Chemother Pharmacol 1998;42: 373–8.
18. Hsu SI, Lothstein L, Horwitz SB. Differential overexpression of three mdr gene family members in multidrug-resistant J774.2 mouse cells. Evidence that distinct P-glycoprotein precursors are encoded by unique mdr genes. J Biol Chem 1989;264:12053–62.
19. Cole SP, Bhardwaj G, Gerlach JH, Mackie JE, Grant CE, Almquist KC, Stewart AJ, Kurz EU, Duncan AM, Deeley RG. Overexpression of a transporter gene in a multidrug-resistant human lung cancer cell line. Science 1992;258:1650–4.
20. Gatti L, Zunino F. Overview of tumor cell chemoresistance mechanisms. Methods Mol Med 2005;111:127–48.
21. Maehara S, Tanaka S, Shimada M, Shirabe K, Saito Y, Takahashi K, Maehara Y. Selenoprotein P, as a predictor for evaluating gemcitabine resistance in human pancreatic cancer cells. Int J Cancer 2004;112: 184–9.
22. Goan YG, Zhou B, Hu E, Mi S, Yen Y. Overexpression of ribonucleotide reductase as a mechanism of resistance to 2,2-difluorodeoxycytidine in the human KB cancer cell line. Cancer Res 1999;59:4204–7.
23. Mosmann T. Rapid colorimetric assay for cellular growth and survival: application to proliferation and cytotoxicity assays. J Immunol Methods 1983;65:55–63.
24. Braakhuis BJ, Ruiz van Haperen VW, Boven E, Veerman G, Peters GJ. Schedule-dependent antitumor effect of gemcitabine in in vivo model system. Semin Oncol 1995;22:42–6.
25. Tsujie M, Nakamori S, Okami J, Hayashi N, Hiraoka N, Nagano H, Dono K, Umeshita K, Sakon M, Monden M. Thiazolidinediones inhibit growth of gastrointestinal, biliary, and pancreatic adenocarcinoma cells through activation of the peroxisome proliferator-activated receptor gamma/retinoid X receptor alpha pathway. Exp Cell Res 2003; 289:143–51.
26. Murata S, Yoshiara T, Lim CR, Sugino M, Kogure M, Ohnuki T, Komurasaki T, Matsubara K. Psychophysiological stress-regulated gene expression in mice. FEBS Lett 2005;579:2137–42.
27. Takemasa I, Higuchi H, Yamamoto H, Sekimoto M, Tomita N, Nakamori S, Matoba R, Monden M, Matsubara K. Construction of preferential cDNA microarray specialized for human colorectal carcinoma: molecular sketch of colorectal cancer. Biochem Biophys Res Commun 2001;285:1244–9.
28. Finke J, Fritzen R, Ternes P, Lange W, Dolken G. An improved strategy and a useful housekeeping gene for RNA analysis from formalin-fixed, paraffin-embedded tissues by PCR. Biotechniques 1993;14: 448–53.
29. Miyamoto A, Nagano H, Sakon M, Fujiwara Y, Sugita Y, Eguchi H, Kondo M, Arai I, Morimoto O, Dono K, Umeshita K, Nakamori S, et al. Clinical application of quantitative analysis for detection of hematogenous spread of hepatocellular carcinoma by real-time PCR. Int J Oncol 2001;18:527–32.
30. Therasse P, Arbuck SG, Eisenhauer EA, Wanders J, Kaplan RS, Rubinstein L, Verweij J, Van Glabbeke M, van Oosterom AT, Christian MC, Gwyther SG. New guidelines to evaluate the response to treatment in solid tumors.European Organization for Research and Treatment of Cancer,National Cancer Institute of the United States,National Cancer Institute of Canada. J Natl Cancer Inst 2000;92:205–16.
31. Wright JA, Chan AK, Choy BK, Hurta RA, McClarty GA, Tagger AY. Regulation and drug resistance mechanisms of mammalian ribonucleotide reductase, and the significance to DNA synthesis. Biochem Cell Biol 1990;68:1364–71.
32. Hurta RA, Wright JA. Alterations in the activity and regulation of mammalian ribonucleotide reductase by chlorambucil, a DNA damaging agent. J Biol Chem 1992;267:7066–71.
33. Heinemann V, Xu YZ, Chubb S, Sen A, Hertel LW, Grindey GB, Plunkett W. Inhibition of ribonucleotide reduction in CCRF-CEM cells by 2′,2′-difluorodeoxycytidine. Mol Pharmacol 1990;38:567–72.
34. Jordan A, Reichard P. Ribonucleotide reductases. Annu Rev Biochem 1998;67:71–98.
35. Xue L, Zhou B, Liu X, Qiu W, Jin Z, Yen Y. Wild-type p53 regulates human ribonucleotide reductase by protein–protein interaction with p53R2 as well as hRRM2 subunits. Cancer Res 2003;63:980–6.
36. Eriksson S, Martin DW, Jr. Ribonucleotide reductase in cultured mouse lymphoma cells. Cell cycle-dependent variation in the activity of subunit protein M2. J Biol Chem 1981;256:9436–40.
37. Guittet O, Hakansson P, Voevodskaya N, Fridd S, Graslund A, Arakawa H, Nakamura Y, Thelander L. Mammalian p53R2 protein forms an active ribonucleotide reductase in vitro with the R1 protein, which is expressed both in resting cells in response to DNA damage and in proliferating cells. J Biol Chem 2001;276:40647–51.
38. Giroux V, Malicet C, Barthet M, Gironella M, Archange C, Dagorn JC, Vasseur S, Iovanna JL. p8 is a new target of gemcitabine in pancreatic cancer cells. Clin Cancer Res 2006;12:235–41.
39. Bepler G, Zheng Z, Gautam A, Sharma S, Cantor A, Sharma A, Cress WD, Kim YC, Rosell R, McBride C, Robinson L, Sommers E, et al. Ribonucleotide reductase M1 gene promoter activity, polymorphisms, population frequencies, and clinical relevance. Lung Cancer 2005;47: 183–92.
40. Jordheim LP, Guittet O, Lepoivre M, Galmarini CM, Dumontet C. Increased expression of the large subunit of ribonucleotide reductase is involved in resistance to gemcitabine in human mammary adenocarcinoma cells. Mol Cancer Ther 2005;4:1268–76.
41. Rosell R, Scagliotti G, Danenberg KD, Lord RV, Bepler G, Novello S, Cooc J, Crino L, Sanchez JJ, Taron M, Boni C, De Marinis F, et al. Transcripts in pretreatment biopsies from a three-arm randomized trial in metastatic non-small-cell lung cancer. Oncogene 2003;22:3548–53.
42. Rosell R, Danenberg KD, Alberola V, Bepler G, Sanchez JJ, Camps C, Provencio M, Isla D, Taron M, Diz P, Artal A. Ribonucleotide reductase messenger RNA expression and survival in gemcitabine/cisplatin-treated advanced non-small cell lung cancer patients. Clin Cancer Res 2004;10:1318–25.

Cancer Chemother Pharmacol (2007) 59:113–126
DOI 10.1007/s00280-006-0250-5

ORIGINAL ARTICLE

Combination therapy of human pancreatic cancer implanted in nude mice by oral fluoropyrimidine anticancer agent (S-1) with interferon-alpha

Kotaro Miyake · Kunihiro Tsuchida · Hiromu Sugino · Satoru Imura · Yuji Morine · Masahiko Fujii · Mitsuo Shimada

Received: 2 February 2006 / Accepted: 27 March 2006 / Published online: 13 May 2006

Abstract *Purpose*: We evaluated the antitumor and antiangiogenic activities of human natural interferon-alpha (IFN-α) alone or in combination with S-1 against human pancreatic cancer cells. *Methods*: Three days after the subcutaneous (s.c.) implantation of tumor cells, mice ($n = 12$) were received s.c. injection with IFN-α alone (10,000 U six times a week), oral administration with S-1 alone (8 mg/kg six times a week), or both with IFN-α and S-1 (8, 10, 12 mg/kg six times a week). *Results*: Administration of IFN-α in combination with S-1 significantly decreased progressive growth and angiogenesis of human pancreatic cancer cells. The combination therapy produced more significant inhibition in expression of the representative pro-angiogenic molecules, vascular endothelial growth factor and basic fibroblast growth factor than individual treatment either IFN-α or S-1 alone did. These treatments also decreased the staining of proliferating cell nuclear antigen, induced apoptosis and decreased microvessel density. In order to better understand the precise molecular mechanisms by which IFN-α and S-1 exert its effects, we have utilized cDNA microarray including 124 known genes to determine the gene expression profile altered by IFN-α and S-1 treatment. We found a total of seven genes which showed a two-fold change after IFN-α and S-1 treatment in addition to VEGF, bFGF, CD31, MMP-2, MMP-7 and MMP-9. Among these genes, we found down-regulation of six genes and up-regulation of one gene, which are related to angiogenesis, tumor cell invasion and metastasis. *Conclusions*: These data suggest that administration of IFN-α in combination with S-1 may provide a novel and effective approach to the treatment of human pancreatic cancer.

Keywords Angiogenesis · DNA microarray · Antitumor effect · S-1 · Interferon-alpha · Pancreatic cancer

K. Miyake · S. Imura · Y. Morine · M. Fujii · M. Shimada (✉)
Department of Digestive and Pediatric Surgery,
Institute of Health Biosciences,
The University of Tokushima Graduate School,
3-18-15 Kuramoto, Tokushima 770-8503, Japan
e-mail: mshimada@clin.med.tokushima-u.ac.jp

K. Tsuchida
Division for Therapies against Intractable Diseases,
Institute for Comprehensive Medical Science (ICMS),
Fujita Health University, Toyoake, 470-1192 Aichi, Japan

H. Sugino
Division of Molecular Cytology,
Institute for Enzyme Research,
The University of Tokushima,
Tokushima 770-8503, Japan

Introduction

Exocrine pancreatic cancer is now the fifth leading cause of cancer death in the USA, Japan, and Europe [1]. Recent advances in the multimodality management of pancreatic cancer have lowered the mortality rates and improved the survival after surgery. However, the overall 1-year survival rate after diagnosis of pancreatic cancer remains below 20%, and the overall 5-year survival rate is only 3%, with the majority of patients dying of metastatic cancer recurrence [2]. Therefore,

new agents and innovative approach to therapy are the important subjects for research.

Among the candidates are the IFNs, a family of natural glycoproteins first discovered in the 1950s due to their antiviral activity [3]. Subsequent studies concluded that the IFNs are multifunctional and can modulate the activities of regulatory cytokines involved in the control of cell function and replication [4–6]. IFN-α has been shown to directly inhibit the proliferation of tumor cells of various histological origins [4–7]. More recently, IFN-α has been shown to down-regulate the expression of the proangiogenic molecules bFGF [8], IL-8 [9], and MMP-2 and -9 [10] and to activate host effector cells [11].

Another candidate, S-1 is a novel oral fluoropyrimidine derivative consisting of tegafur (FT) and two modulators, 5-chloro-2,4-dihydroxypyridine (CDHP) and potassium oxonate (Oxo), in a molar ratio of 1:0.4:1 [12]. Antitumor effect is provided by the 5-fluorouracil (5-FU) prodrug FT [13]. CDHP competitively inhibits the 5-FU degradative enzyme dihydropyrimidine dehydrogenase (DPD), resulting in the retention of a prolonged concentration of 5-FU in blood [14]. Oxo competitively inhibits orotate phosphoribosyltransferase, which converts 5-FU to 5-fluorouridine 5′-monophosphate in vitro [15]. Because Oxo is mainly distributed in the gastrointestinal tract after oral administration, it acts to relieve the gastrointestinal toxicity induced by 5-FU. Recent clinical trials using S-1 have shown promising results in various solid tumors. Response rates of 35–50% were reported for single agent or combination of S-1 and other anticancer drug use for gastric cancer [16], colon cancer [17], and pancreatic cancer [18].

The combination therapy of IFN-α and 5-FU was initially proposed in 1988 based on in vitro experiments on colon cancer cells [19]. Subsequently, this combination therapy was applied to various types of human carcinomas. In the clinical studies, outstanding effects with IFN-α and 5-FU therapy were observed in patients with advanced HCC [20]. Several in vitro studies have provided some explanations about the synergistic effects of the combination of IFN-α and 5-FU [21–23].

The aim of this study was to determine the therapeutic effect of IFN-α in combination with S-1 against the pancreatic cancer AsPC-1 implanted in athymic nude mice [24]. We show that the combination of IFN-α and S-1 administration significantly inhibited the growth of human pancreatic cancer by down-regulating the expression of VEGF and bFGF, by inducing apoptosis in tumor cells and by inhibiting tumor cell proliferation.

Materials and methods

Cell lines and culture conditions

AsPC-1, MIA PaCa-2, BxPC-3 and PANC-1 cells were purchased from the Japanese Collection Research Bioresources Cell Bank (Tokyo, Japan). All cell lines were grown in RPMI 1640 supplemented with 10% fetal bovine serum (FBS), 70 μg/mL penicillin and 100 μg/mL streptomycin (complete medium) and maintained at 37°C in a humidified incubator with 5% CO_2 in air. The cultures were maintained for no longer than 12 weeks after recovery from frozen stock.

Reagents

Human natural IFN-α (BALL1) was purchased from Otsuka Pharmaceutical Co. (Tokushima, Japan) and was kept at 4°C and diluted in 0.1% Tween 80 as necessary at the time of use. 5-FU was purchased from Kyowa Hakko Kogyo, Co., Ltd. (Tokyo, Japan) and dissolved in 0.9% NaCl solution. Tegafur, CDHP, and Oxo were provided by Taiho Pharmaceutical Co., Ltd., Tokyo, Japan. We prepared S-1 by mixing tegafur, CDHP, and Oxo at a molar ratio of 1:0.4:1 in 0.5% (w/v) hydroxypropylmethylcellulose (HPMC) solution. The dose of S-1 is expressed as the dose of tegafur, because the active component of S-1 is tegafur. Antibodies purchased were as follows: polyclonal rabbit anti-VEGF/vascular permeability factor (Santa Cruz Biotechnology, Santa Cruz, CA, USA); peroxidase-conjugated goat anti-rabbit (IgG) $F(ab')_2$ (Jackson Research Laboratories, West Grove, CA, USA); monoclonal rat anti-mouse CD31/PECAM-1 (PharMingen, San Diego, CA, USA); peroxidase-conjugated goat anti-rat IgG (H&L; Jackson Research Laboratories); monoclonal mouse anti-PCNA clone PC-10 (DAKO A/S); peroxidase-conjugated rat anti-mouse IgG2a heavy chain (Serotec; Harlan Bioproducts for Science, Inc., Indianapolis, IN, USA); rabbit anti-human bFGF (Santa Cruz Biotechnology); PBS; goat polyclonal anti-human MMP-2 (Santa Cruz Biotechnology); mouse monoclonal anti-human MMP-7 (Fuji Chemical, Toyama, Japan); rabbit polyclonal anti-human MMP-9 antibody (Oncogene Research Products, Cambridge, MA, USA); peroxidase-conjugated rat anti-mouse IgG1 (PharMingen); stable 3,3′-diaminobenzidine was purchased from Research Genetics (Huntsville, AL, USA) and Gill's hematoxylin was purchased from Sigma. Pepsin was purchased from Biomeda (Foster City, CA, USA). The Cell Counting Kit-8 using WST-8(2-(2-methoxy-4-nitrophenyl)-3-(4-nitrophenyl)-5-(2,4-disulfophenyl)-2H-tetrazolium,

monosodium salt) was purchased from Wako (Osaka, Japan). The TUNEL assay was performed using a commercial apoptosis detection kit (Promega, Madison, WI, USA) with modifications.

Cell proliferation assay

All of tumor cells (5×10^3) were seeded into 38-mm^2 wells of flat-bottomed 96-well plates in quadriplicate and allowed to adhere overnight. The spent medium was then removed, and the cultures were refed with new medium (negative control) or medium containing different concentrations of human IFN-α and S-1. Incubation was continued for 96 h prior to adding the Cell Counting Kit-8, and after 4 h, the optical density was measured at 450 nm with a microplate reader (Multiskan JX; Labsystems). The WST-8 assay correlated with the results obtained by cell counting with a hemocytometer [25]. Assays were performed in quadruplicate in duplicate plates.

Animals study

Since AsPC-1 cells rapidly form a tumor when inoculated in the subcutaneous space of nude mice, we used the cells in an in vivo model. Female athymic nude mice (NCI-nu) were purchased from CLEA Japan, Co. Ltd (Tokyo, Japan). The mice were maintained under specific pathogen-free conditions in facilities approved by the animal experimental institutional of the University of Tokushima. The mice were used in accordance with animal experimental institutional policy of the University of Tokushima when they were 4–5 weeks old. Tumor sizes were measured with a caliper every week. The tumor volume was calculated using the formula: Volume = $S \times S \times L/2$, where S is the short length of the tumor in centimeter and L is the long length of the tumor in centimeter.

To produce pancreatic tumors in nude mice, the AsPC-1 cells were harvested from subconfluent cultures by a brief exposure to 0.25% trypsin and 0.02% EDTA. Trypsinization was stopped with medium containing 10% fetal bovine serum, and the cells were washed once in serum-free medium and resuspended in PBS. Only suspensions consisting of single cells with > 90% viability were used for the injections. Cells were injected into the subcutaneous tissue as described previously [26]. The mice were killed when moribund. The size and weight of the primary pancreatic tumors were recorded. Histopathology confirmed the nature of the disease. For histology and immunohistochemistry, one part of the tumor tissue was fixed in formalin and embedded in paraffin. Another part of the tumor was embedded in OCT compound (Miles, Inc., Elkhart, IN, USA), snap frozen in liquid nitrogen, and stored at −70°C.

Therapy of established human pancreatic carcinoma tumors growing in nude mice

Three days after the implantation of tumor cells into the subcutaneous tissue, for the first experiment, the mice were randomized into the following three treatment groups, ($n = 6$): (1) control, (2) thrice a week s.c. administrations of IFN-α (23,000 U), (3) six times a week s.c. administration of human IFN-α (10,000 U). Control mice were received s.c. PBS (vehicle). The mice were necropsied on day 35, and the volume of pancreatic tumors were recorded. In the same way, the second experiment was performed, and the mice were randomized into the following five treatment groups ($n = 6$): (1) control, (2) six times a week administrations of S-1 (6 mg/kg), (3) six times a week administrations of S-1 (8 mg/kg), (4) six times a week administrations of S-1 (10 mg/kg), (5) six times a week administrations of S-1 (12 mg/kg). Control mice were received HPMC solution (vehicle). The mice were necropsied on day 35, and the results were analyzed as described earlier. In the third experiment, the effective dosage of IFN-α as determined in the first experiment and S-1 in the second experiment was used. Six treatment groups ($n = 12$) were used as follows: (1) control, (2) six times a week s.c. administration of human IFN-α (10,000 U) alone, (3) six times a week administrations of S-1 (8 mg/kg) alone, (4) six times a week administration of IFN-α (10,000 U) and S-1 (8 mg/kg), (5) six times a week administration of IFN-α (10,000 U) and S-1 (10 mg/kg), (6) six times a week administration of IFN-α (10,000 U) and S-1 (12 mg/kg). The control mice received PBS and HPMC solution (vehicle). The mice were necropsied on day 35, and the results were analyzed as described earlier.

Survival assay in nude mice

Aliquots of cells (1×10^6) were suspended in 50 μl of PBS as single-cell suspensions. Nude mice were anesthetized with methoxyflurane and placed in the supine position. An upper midline abdomen incision was made, and the pancreas was exteriorized. Tumor cells were injected into the tail of the pancreas, and the abdomen was closed using wound clips. Mice received implant of AsPC-1 cells in the pancreas and were randomized on day 7 to the four groups ($n = 5$). Tumors in the pancreas were harvested and weighed. For survival assays, daily survival of mice was monitored and

recorded as dead or euthanized when the animals reached the moribund stage.

Necropsy procedures

The mice were killed, and body weight was determined. Primary tumors in the subcutaneous tissue were excised, measured, and weighed.

Immunohistochemical analysis

Paraffin-embedded tissues were used for IHC identification of VEGF, bFGF, MMP-2, MMP-7, MMP-9, and PCNA. Sections (4–6 μm thick) were mounted on positively charged Superfrost slides (Muto Pure Chemicals Co., Ltd.) and dried overnight. Sections were deparaffinized in xylene, followed by treatment with a graded series of alcohol [100, 95, and 80% ethanol/double-distilled H_2O (v/v)] and rehydrated in PBS (pH 7.5). The sections analyzed for bFGF were treated with pepsin (Biomeda) for 15 min at 37°C and washed with PBS. All other paraffin-embedded tissues were microwaved for 10 min for "antigen retrieval." Frozen tissues used for identification of CD31/PECAM-1 were sectioned (8–10 μm), mounted on positively charged Plus slides (MUTO PURE CHEMICALS CO), and air dried for 30 min. Frozen sections were fixed in cold acetone (5 min), acetone/chloroform (v/v; 5 min), and acetone (5 min) and washed with PBS. IHC procedures were performed as described previously [27]. Positive reactions were visualized by incubating the slides with stable 3,3′-diaminobenzidine for 10–20 min. The sections were rinsed with distilled water, counterstained with Gill's hematoxylin for 30 s, and mounted with Universal Mount (Research Genetics). Control samples exposed to secondary antibody alone showed no specific staining.

TUNEL staining

TUNEL was performed using a commercially available apoptosis detection kit with the following modifications: samples were fixed with 4% paraformaldehyde (methanol-free) for 10 min at room temperature; washed twice with PBS for 5 min; and then incubated with 0.2% Triton X-100 for 15 min at room temperature. After being washed twice (5 min/each) with PBS, the samples were incubated with equilibration buffer containing 200 mM potassium cacodylate (pH 6.6), 25 mM Tris–HCl (pH 6.6), 0.2 mM DTT, 0.25 mg/ml BSA, and 2.5 mM cobalt choloride, for 10 min at room temperature. The equilibration buffer was drained, and reaction buffer containing equilibration buffer, nucleotide mix, and terminal deoxynucleotidyl transferase enzyme was added to the tissue sections and incubated in a humidified chamber at 37°C for 1 h in the dark. Immersing the samples in 2 × SSC for 15 min terminated the reaction, and samples were washed 3 times for 5 min to remove unincorporated fluorescein-dUTP. For quantification of endothelial cells, the samples were incubated with 300 μg/ml Hoechst dye for 10 min at room temperature. Fluorescent bleaching was minimized by treating slides with an enhancing reagent (Prolong solution). Immunofluorescence microscopy was performed using a × 20 objective (Carl ZEISS, Axioplan2) on an epifluorescence microscope equipped with UV filter wheel. Images were captured using a DIGITAL CAMERA: Dxm1200 (Nikon, Tokyo, Japan). Images were further processed using Adobe Photoshop software (Adobe Systems, Mountain View, CA, USA). DNA fragmentation was detected by localized green fluorescence within the nucleus (visualized by Hoechst stain) of apoptotic cells. For the quantification of total TUNEL expression, the number of apoptotic events was counted in five random fields at × 200 magnification.

Quantification of microvessel density (MVD) and PCNA

For the quantification of MVD, five random 0.95 mm^2 fields at × 200 magnification were captured for each tumor, and microvessels were quantified according to the method previously described [27, 28]. For the quantification of PCNA expression, the number of positive cells was quantified in five random fields at × 200 magnification.

Thymidylate synthase (TS) activity

For TS and DPD activity assay, tumor tissue was harvested on day 35 of treatment. The TS content was determined as the quantity of [6-^{3}H]-FdUMP binding sites in the 105,000 g supernatant (cytosol) of tumor tissue homogenates, based on the method described by Spears et al. [29], with minor modifications [30]. The samples for TS total were prepared by causing the ternary complex present in the cytosol to be fully dissociated to unbound TS at pH 8.0 during the preincubation period. In the case of TS-free samples, pre-incubation for the dissociation process was omitted. TS total and TS-free samples were incubated with [6-^{3}H]-FdUMP in the presence of 5,10-methylenetetrahydrofolate for 20 min at 30°C, and radioactivity in the acid-insoluble fraction was measured with a liquid scintillation counter. Protein concentration was determined using a

protein assay kit (Bio-Rad, Richmond, CA, USA). The TS content is expressed as pmol/mg of protein.

Dihydropyrimidine dehydrogenase (DPD) activity

Dihydropyrimidine dehydrogenase activity was measured according to the procedures of Takechi et al. [31], with minor modifications [30]. Briefly, enzyme solution obtained from a tumor was incubated with reaction mixture containing 2 mM dithiothreitol, 5 mM $MgCl_2$, 20 mM [6-^{14}C]-FU (56 nCi), and 100 mM NADPH at 37°C for 10 or 30 min. The reaction mixture was boiled and centrifuged. The mixture was centrifuged at 1,500*g* for 10 min, and the supernatant was then incubated with 0.36 M KOH at room temperature for 30 min. The solution was then mixed with 0.36 M $HClO_4$ and centrifuged at 1500*g* for 10 min. An aliquot of supernatant was applied to a thinlayer chromatography plate (silica gel 60 F254, Merck, Darmstadt, Germany), which was then developed with a mixture of 99% ethanol and 1 M ammonium acetate (5:1, v/v). The plate was then read on an imaging analyzer (Bio-Rad), and the densities of 5-FU and the degradation products were calculated. DPD activity was expressed as pmol/mg protein/min.

Customized DNA array

Two customized DNA arrays have been developed to measure molecular markers, involved in response to the 5-FU and other anticancer drugs-related genes, and metastasis and invasion-related genes. A total of 52 and 72 genes are shown in Tables 1 and 2. The first one consists of 25 genes related to pyrimidine/purine/folate metabolism (ex. thymidylate synthase, dihydropyrimidine dehydrogenase, etc.), 9 genes related to DNA repair (e.g. DNA ligase I, uracil-DNA glycosylase, etc.), 8 genes related to drug resistance (P-glycoprotein, topoisomerase 1, etc.), 7 other genes (p53, proliferating cyclic nuclear antigen, etc.) and 3 housekeeping genes (glyceraldehyde-3-phosphate dehydrogenase, beta-actin, 40S ribosomal protein S9). The second one consists of 71 genes related to metastasis and invasion and 1 housekeeping gene (beta-actin). Target DNAs made from the 52 and 72 genes were immobilized on a glass plate, respectively. Each target DNA (200–600 bp) was designed based on sequence homology analysis to minimize cross-hybridization with other genes, and was practically tested by Northern blot. All genes could be relatively determined in a single assay. The basic technology of the customized DNA array is almost the same as that of a Stanford-type cDNA microarray (Dr Brown's Lab protocol, http://www.cmgm.stanford.edu/pbrown/protocols/index.html). Samples of the tumors which were resected from the subcutaneously implanted nude mice were stored at −80°C until use. Frozen tissues were suspended in Buffer RLT (Qiagen, Hilden, Germany) and homogenized using a Mixer Mill MM300 (F. Kurt Retsch GmbH & Co., Haan, Germany). RNA extraction was performed using an RNeasy mini kit (Qiagen, Hilden, Germany). Total RNA quality was judged from the relative intensities of the 28S and 18S ribosomal RNA bands after agarose gel electrophoresis. Purified total RNA (20 μg) was incubated at 70°C for 5 min and cooled on ice. It was reverse-transcribed with a mixture of specific primers and 200 U of PowerScript reverse transcriptase, and incubated at 42°C for 1.5 h. The cDNA was labeled using Cy5 (Cy5 monofunctional reactive dye, Amersham, Cat. no. PA25001), and purified by a Nucleo Spin Extract kit (Macherey-Nagel GmbH & Co. KG, Dueren, Germany). Labeled cDNA was hybridized in 6 × SSC, 0.2% SDS, 0.01 mg/ml Human Cot-1 DNA and 5 × Denhalt's solution for 16 h at 60°C for spotted cDNA arrays. The slides were washed in 2 × SSC at room temperature, then 2 × SSC with 0.2% SDS at 55–65°C twice, and finally 0.05 × SSC at room temperature and scanned using a Scanner FLA-8000 (FujiFilm, Tokyo, Japan). Data were analyzed using an Array Gauge (FujiFilm, Tokyo, Japan) by Taiho Pharmaceutical Co. Ltd., Tokyo, Japan. When, by fold change, transcripts increased or decreased twofold, it was considered differentially expressed.

Statistical analysis

Pancreatic tumor volume was compared using the Mann–Whitney *U* test. Quantification of PCNA, TUNEL, CD31, and the number of apoptotic endothelial cells were compared by the Mann–Whitney *U* test. Survival analysis was computed by the Kaplan–Meier method and compared by the log-rank test. Statistical analysis was performed using StatView 5.0J software (SAS Institute, Inc., Cary, NC, USA). A *P* value of less than 0.05 was considered to be statistically significant.

Results

Growth inhibition assay by IFN-α and/or S-1

We tested the dose-dependent cell growth suppression of IFN-α or S-1 treatment on several human pancreatic cancer cell lines. The growth of cell lines were suppressed by IFN-α or S-1. To examine whether

Table 1 Fifty-two genes were examined using customized cDNA array

No.	Gene name	Abbreviated name	GenBank accession
1	Equilibrative nucleoside transporter 1	ENT1	NM_004955
2	Equilibrative nucleoside transporter 2	ENT2	AF034102
3	P-glycoprotein	MDR1	NM_000927
4	Multidrug resistance-associated protein 1	MRP1	L05628
5	Heat shock protein 27	Hsp27	NM_001540
6	Topoisomerase 1	TOP1	J03250
7	Topoisomerase 2 alpha	TOP2A	NM_001067
8	Topoisomerase 2 beta	TOP2B	X68060
9	Thymidylate synthase	TS	NM_001071
10	Dihydropynmidine dehydrogenase	DPD	U09178
11	Thymidine phosphorylase	TP	M63193
12	Uridine phosphorylase	UP	NM_003364
13	Orotate phosphoribosyltransferase	OPRT	NM_000373
14	Ribonucleoside-diphosphate reductase M1 subunit	RRM1	X59543
15	Ribonucleoside-diphosphate reductase M2 subunit	RRM2	NM_001034
16	Thymidine kinase, soluble	TK1	NM_003258
17	Uridine cytidine kinase 2	UCK2	AF236637
18	Nucleosie diphosphate kinase A	NDKA	X17620
19	Nucleosie diphosphate kinase B	NDKB	L16785
20	Cytidine deaminase	CDA	L27943
21	Deoxycytidine kinase	DCK	NM_000788
22	RNA polymerase 2	RP2	NM_000937
23	Uridine monophosphate kinase	UMPK	NM_016308
24	5′ Nucleotidase	NT5	NM_002526
25	Deoxycytidylate deaminase	DCD	NM_001921
26	CTP synthase	CTPS	NM_001905
27	IMP dehydrogenase 1	IMPD	NM_000883
28	Adenine phosphonbosyltransferase	APRT	NM_000485
29	Adenosine kinase	AK	U33936
30	Phosphonbosyl pyrophosphate synthetase	PRPS	D00860
31	Hypoxanthine phosphonbosyltransferase 1	HPRT1	NM_000194
32	Methylenetetrahydrofolate dehydrogenase	MTHFD1	NM_005956
33	Folylpolyghutamate synthetase	FPGS	NM_004957
34	Uracil-DNA glycosylase	UDG	X15653
35	Poly (ADP-ribose) polymerase	PARP	NM_001618
36	DNA ligase I	LIG1	NM_000234
37	DNA ligase III	LIG3	X84740
38	DNA ligase IV	LIG4	NM_002312
39	DNA excision repair protein ERCCÇP	ERCC1	NM_001983
40	DNA repair protein XRCC1	XRCC1	NM_006297
41	DNA polymerase b	POLB	NM_002690
42	DNA polymerase d	POLD	NM_002691
43	Glyceraldehyde-3-phosphate dehydrogenase	GAPDH	X01677
44	Beta-actin	ACTB	NM_001101
45	40S ribosomal protein S9	RSP9	U14971
46	Proliferating cyclic nuclear antigen	PCNA	NM_002592
47	VEGF beta	VEGFB	U48801
48	Integin alpha 3	ITGA3	NM_002204
49	p53	p53	NM_000546
50	E2F1	E2F1	M96577
51	CuZn SOD	SOD1	X02317
52	Mn SOD	SOD2	NM_000636

combination therapy have cooperative effects on cell growth inhibition, cells were exposed to IFN-α and S-1 for 96 h at various concentrations. The exposure of cells to a combination of IFN-α and S-1 synergistically suppressed cell growth (Fig. 1).

Inhibition of pancreatic cancer growth

The first experiment was carried out to determine the dose of IFN-α. AsPC-1 cells were injected into the subcutaneous tissue of athymic nude mice. After 3 days, the

Table 2 Seventy-one genes were examined using customized cDNA array

No.	Gene name	Abbreviated name	GenBank accession
1	Beta actin	ACTB	NM_001101
2	Autocrine motility factor receptor	AMFR	NM_001144
3	Fibroblast growth factor 2	FGF2	NM_002006
4	Cathepsin B preproprotein	CTSB	NM_001908
5	Platelet endothelial cell adhesion molecule 1	PECAM1	NM_000442
6	CD34 antigen	CD34	NM_001773
7	Cadherin I. type 1	CDH1	NM_004360
8	Epidermal growth factor receptor	EGFR	NM_005228
9	v-ets erythroblastosis virus E26 oncogene	ETS1	NM_005238
10	Fms-related tyrosine kinase 1	FLT1	NM_002019
11	Fms-related tyrosine kinase 4	FLT4	NM_182925
12	v-fos FBJ murine ostesarcoma viral oncogene	FOS	NM_005252
13	Kinase insert domain receptor	KDR	NM_002253
14	Matrix metalloproteinase 1	MMP1	NM_002421
15	Matrix metalloproteinase 2	MMP2	NM_004530
16	Matrix metalloproteinase 3	MMP3	NM_002422
17	Matrix metalloproteinase 7	MMP7	NM_002423
18	Matrix metalloproteinase 9	MMP9	NM_004994
19	Met proto-oncogene	MET	NM_000245
20	Matrix metalloproteinase 14	MMP14	NM_004995
21	Matrix metalloproteinase 16	MMP16	NM_022564
22	v-myc myelocytomatosis viral oneogene	MYC	NM_002467
23	v-rel reticuloendotheliosis viral oncogene	RELA	NM_021975
24	Nucleoside-diphosphate kinase 1	NME1	NM_000269
25	Nucleoside-diphosphate kinase 2	NME2	NM_002512
26	Plasminogen activator inhibitor-1	SERPINE1	NM_000602
27	Serine proteinase inhibitor, clade B, member 2	SERPINB2	NM_002575
28	Transferrin receptor	TFRC	NM_003234
29	Transforming growth factor, alpha	TGFA	NM_003236
30	Transforming growth factor, beta 1	TGFB1	NM_000660
31	Transforming growth factor, beta 2	TGFB2	NM_003238
32	Transforming growth factor, beta 3	TGFB3	NM_003239
33	Transforming growth factor, beta receptor III	TGFBR3	NM_003243
34	Tyrosine kinase with immunoglobulinand epidermal growth factor	TIE	NM_005424
35	TEK tyrosine kinase, endothelial	TEK	NM_000459
36	Plasminogen activator, urokinase	PLAU	NM_002658
37	Plasminogen activator, urokinase receptor	PLAUR	NM_002659
38	Vascular endothelial growth factor	VEGF	NM_003376
39	Vascular endothelial growth factor C	VEGFC	NM_005429
40	Lintegrin alpha 2	ITGA2	NM_002203
41	Integrin alpha 3	ITGA3	NM_002204
42	Integrin alpha 4	ITGA4	NM_000885
43	Integrin alpha 5	ITGA5	NM_002205
44	Integrin alpha chain, alpha 6	ITGA6	NM_000210
45	Catenin (cadherin-associated protein), alpha 1	CTNNA1	NM_001903
46	Integrin, alpha V	ITGAV	NM_002210
47	Thrombospondin 1	THBS1	NM_003246
48	Integrin beta 1	ITGB1	NM_002211
49	Integrinbeta chain, beta 3	ITGB3	NM_000212
50	Integrin, beta 5	ITGB5	NM_002213
51	Catenin (cadherin-associated protein), beta 1	CINNB1	NM_001904
52	S-adenosylhomocysteine hydrolase	AHCY	NM_000687
53	Cystathionine-beta-synthase	CBS	NM_000071
54	DNA (cytosine-5-)-methyltransferase 1	DNMT1	NM_001379
55	DNA cytosine methyltransferase 3 alpha	DNMT3A	NM_175629
56	Histone deacetylase 1	HDAC1	NM_004964
57	Histone deacetylase 2	HDAC2	NM_001527
58	Histone deacetylase 3	HDAC3	NM_003883
59	Histone deacetylase 4	HDAC4	NM_006037
60	Histone deacetylase 5	HDAC5	NM_005474
61	Histone deacetylase 6	HDAC6	NM_006044
62	Methionine adenosyltransferase I, alpha	MAT1A	NM_000429

Table 2 continued

No.	Gene name	Abbreviated name	GenBank accession
63	Methionine adenosyltransferase II, alpha	MAT2A	NM_005911
64	Methionine adenosyltransferase II, beta	MAT2B	NM_013283
65	Methyl-CpG binding domain protein 2	MBD2	NM_003927
66	Methyl-CpG binding domain protein 3	MBD3	NM_003926
67	Methyl-CpG binding domain protein 4	MBD4	NM_003925
68	Methyl CpG binding protein 2	MECP2	NM_004992
69	5,10-Methylenetetrahydrofolate reductase	MTHFR	NM_005957
70	5-Methyltetrahydrofolate-homocysteine methyltransferase	MTR	NM_000254
71	Cathespin L	CTSL	NM_001912
72	Angiopoietin 2	ANGPT2	NM_001147

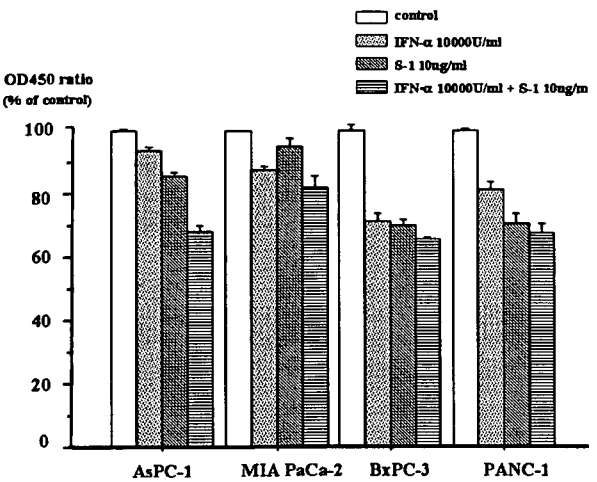

Fig. 1 Effect of IFN-α and/or S-1 on in vitro growth of pancreatic cancer cells. Pancreatic cancer cells were seeded in 96-well plates (5.0×10^3 cells/well), and then incubated for 96 h in RPMI1640 medium in the absence or presence of IFN-α and/or S-1. Live cells were determined by the Cell Counting Kit-8. Results are expressed as the percentages of live cells compared with those without IFN-α and/or S-1 treatment. The *error bars* indicate the standard deviation (*$P < 0.05$ vs. control and single-agent therapy)

mice were randomized into three groups of six mice each. The first group received human IFN-α at 23,000 U s.c. three times a week, the second group received human IFN-α at 10,000 U s.c. six times a week, and the third group (control) received 0.1% Tween 80 s.c. All mice were killed on day 35. As shown in Fig. 2a, daily s.c. injections of IFN-α (10,000 U) had a tendency to decrease median tumor volume as compared with control mice.

The second experiment was carried out to determine the dose of S-1. The first group received S-1 at 6 mg/kg by a gastric tube six times a week, the second group received S-1 at 8 mg/kg six times a week, the third group received S-1 at 10 mg/kg six times a week, the fourth group received S-1 at 12 mg/kg six times a week, and the sixth group (control) received 0.1% HPMC. All mice were killed on day 35. As shown in Fig. 2b, daily oral administration of S-1 (10, 12 mg/kg) also had a tendency to decrease median tumor volume as compared with control mice.

The third experiment was carried out using IFN-α (10,000 U, s.c.), S-1 (8 mg, oral administration), and IFN-α (10,000 U) plus S-1 (8, 10, 12 mg/kg) six times a week. As shown in Fig. 2c, the mean tumor volume was $1{,}004 \pm 367$ mm^3 in control, 974 ± 556 mm^3 in IFN-α alone 844 ± 297 mm^3 in S-1 alone, 538 ± 134 mm^3 in combination of IFN-α and S-1 (8 mg/kg), 444 ± 166 mm^3 in combination of IFN-α and S-1 (10 mg/kg) and 264 ± 113 mm^3 in combination of IFN-α and S-1 (12 mg/kg).

The daily s.c. injections of IFN-α and oral administration of S-1 (12 mg/kg) significantly decreased median tumor volume, as compared with control, IFN-α alone, S-1 alone, and combination of IFN-α and S-1 (8 mg) mice. Treatments with IFN-α alone or in combination with S-1 were well tolerated as determined by maintenance of body weight.

Survival assays in nude mice

Survival assays were carried out to determine survival using orthotopic model. The mice were killed and necropsied only when they became moribund. The median survival time for the control group was 28 days. After treatment with IFN-α alone, S-1 alone, and a combination of IFN-α and S-1 (8, 10, 12 mg/kg), the median survival time was 57, 51, 48, 48, and 48 days, respectively (control vs. IFN-α, $P < 0.01$; control versus S-1, $P < 0.05$; control vs. IFN-α and S-1 (8 mg/kg), $P < 0.05$; control vs. IFN-α and S-1 (10 mg/kg), $P = 0.11$; control vs. IFN-α and S-1 (12 mg/kg), $P = 0.09$; Fig. 3).

Immunohistochemical analysis of VEGF, bFGF, CD31/PECAM-1, and PCNA

We next determined the in vivo effects of IFN-α alone or in combination with S-1. At 35 days of treatment,

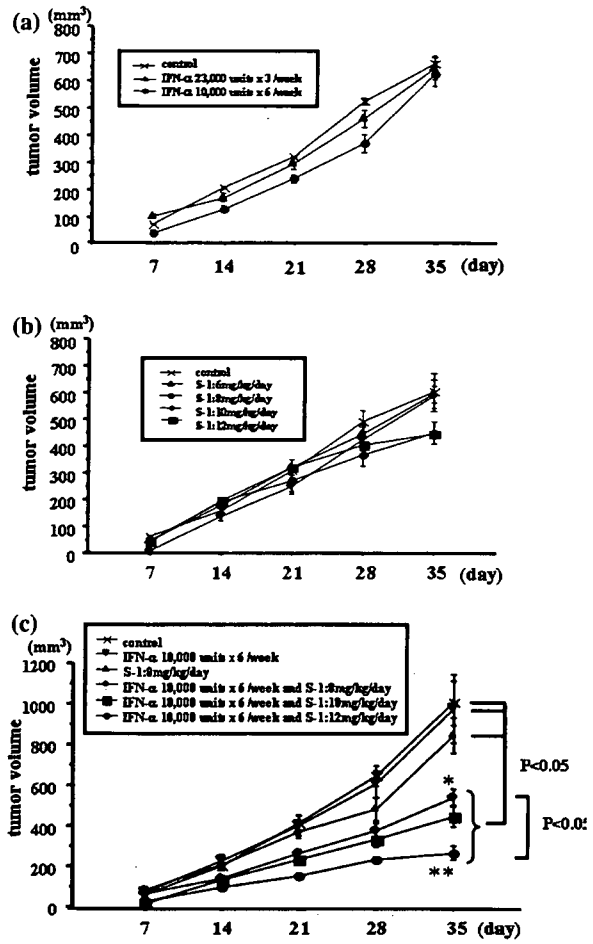

Fig. 2 a Effect of IFN-α on AsPC-1 xenografts growth. Mice were given 10,000 or 23,000 U IFN-α s.c. injections three or six times a week. Tumor volume was measured weekly. Each experiment was performed using six mice. *Error bars* represent the standard deviation (*cross* control; *filled triangle* 23,000 U, three times a week; *filled circle* 10,000 U, six times a week). **b** Effect of S-1 on AsPC-1 xenografts. Mice were given oral doses of 6, 8, 10, 12 mg/kg S-1 on 6 consecutive days. S-1 is administrated by a gastric tube. Tumor volume was measured weekly. Each experiment was performed using six mice. *Error bars* represent the standard deviation. (*cross* Control; *filled triangle* 6 mg/kg; *filled circle* 8 mg/kg; *filled diamond* 10 mg/kg; *filled square* 12 mg/kg). **c** Combined effects of IFN-α and S-1 on AsPC-1 xenografts growth. Mice were given 10,000 U IFN-α s.c. injections and/or oral doses of 8, 10, 12 mg/kg S-1 on 6 consecutive days. Tumor volume was measured weekly. Each experiment was performed using 12 mice. *Error bars* represent the standard deviation. (*cross* Control; *inverted triangle* IFN-α only; *filled triangle* S-1 only; *filled diamond* IFN-α and S-1(8 mg/kg); *filled square* IFN-α and S-1(10 mg/kg); *filled circle* IFN-α and S-1 (12 mg/kg) (*$P < 0.05$ vs. control and single-agent therapy; **$P < 0.05$ vs. IFN-α and S-1 (8 mg/kg))

all mice were killed and necropsied, and tumors were harvested and processed for routine histology, and IHC analyses of cell proliferation and apoptosis using anti-PCNA antibodies and the TUNEL method, respectively.

At 35 days of treatment, the mean number of $PCNA^+$ tumor cells in control tumors was 906 ± 137. After therapy with IFN-α or S-1, the mean number was 608 ± 105 or 570 ± 93, respectively. The lowest number of $PCNA^+$ cells (330 ± 109) was found in tumors of mice treated with both IFN-α and S-1 ($P < 0.01$ vs. other treatment groups) (Fig. 4, Table 3).

The mean number of $TUNEL^+$ cells was inversely related to PCNA positivity. The mean number of $TUNEL^+$ cells was 7 ± 4 in control tumors, 14 ± 3 in IFN-α-treated tumors, 25 ± 18 in S-1-treated tumors, and 49 ± 13 in IFN-α and S-1-treated tumors (control vs. S-1, $P = 0.06$; control vs. IFN-α, $P < 0.05$; control vs. IFN-α and S-1, $P < 0.0001$). In the combination therapy group, the number of $TUNEL^+$ tumor cells significantly increased as compared with other group tumors ($P < 0.05$; Fig. 4, Table 3).

The mean number of MVD (measured by staining with antibodies against CD31) cells was 26 ± 5 in control tumors, 13 ± 2 in IFN-α-treated tumors, 19 ± 3 in S-1-treated tumors, and 11 ± 3 in IFN-α and S-1-treated tumors There was a significant reduction in tumor MVD per field after treatment with IFN-α or combination therapy as compared with control tumors

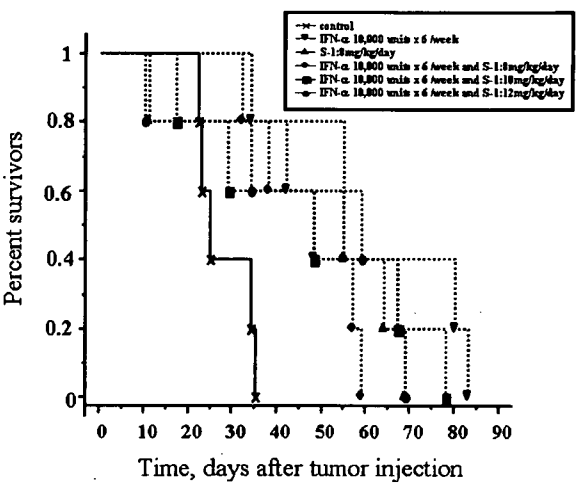

Fig. 3 Therapeutic effects of IFN-α and S-1. AsPC-1 cells were injected in the pancreas of nude mice. Seven days later, the mice were randomized into four treatment groups ($n = 5$). Mice were killed when moribund. Survival was analyzed by the Kaplan–Meier method and compared by the log-rank test. *Cross* Control; *filled inverted triangle* IFN-α only; *filled triangle* S-1 only; *filled diamond* IFN-α and S-1 (8 mg/kg); *filled square* IFN-α and S-1 (10 mg/kg); *filled circle* IFN-α and S-1 (12 mg/kg) (control vs. IFN-α, $P < 0.01$; control vs. S-1, $P < 0.05$; control vs. IFN-α and S-1 (8 mg/kg), $P < 0.05$; control vs. IFN-α and S-1 (10 mg/kg), $P = 0.11$; control vs. IFN-α and S-1 (12 mg/kg), $P = 0.09$)

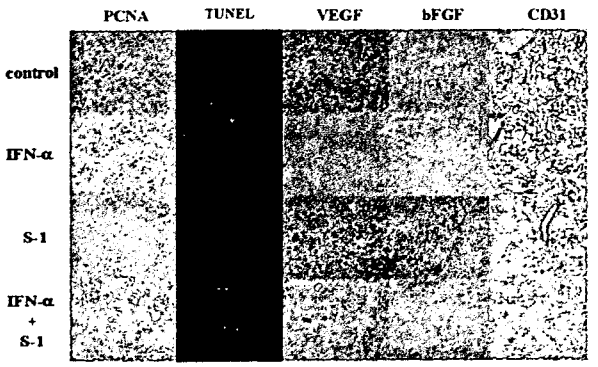

Fig. 4 Effects of IFN-α and S-1 detected by immunohistochemical analysis. Tumors were harvested from control mice and mice treated with IFN-α, S-1, or both. The sections were immunostained for expression of PCNA (to show cell proliferation), TUNEL (FITC; to show cell death), VEGF, bFGF, and CD31. Tumors from mice treated with IFN-α and S-1 had a decrease in $PCNA^+$ cells, VEGF, bFGF, and CD31 staining, an increase in $TUNEL^+$ cells. *Representative samples* (× 200) are shown

Table 3 Immunohistochemical analysis of human pancreatic carcinoma in the control and treated mice

Treatment group[a]	$PCNA^+$	$TUNEL^+$	$CD31^+$
Control	906 ± 137^b	7 ± 4^b	26 ± 5^b
IFN-α	608 ± 105^c	14 ± 3	13 ± 2^e
S-1	570 ± 93	25 ± 5	19 ± 3^e
IFN-α and S-1	330 ± 109^d	49 ± 5^d	11 ± 3^e

[a] AsPC-1 human pancreatic cancer cells (1×10^6) were injected into the subcutaneous of nude mice. Three days later, groups of mice were treated with daily s.c. injections of IFN-α (10,000 U) alone, daily s.c. injections of human IFN-α (10,000 U) alone, daily oral admistration S-1(12 mg/kg) alone, or with IFN-α and S-1 or saline (control)

[b] Number (mean ± SD) if CD31, PCNA positive cells/field determined from measurement of 5 random 0.95 mm^2 fields at 200× magnification

[c] $P < 0.05$ as compared with controls

[d] $P < 0.05$ as compared with single-agent therapy

[e] $P < 0.05$ as compared with S-1 therapy

or S-1-treated tumors ($P < 0.05$). There was no significant difference between MVD of tumors treated with IFN-α and MVD of tumors from mice given combination therapy ($P = 0.2$; Fig. 4, Table 3).

The IHC staining of tumors after 35 days of treatment with IFN-α and S-1 revealed a significant decrease in expression of VEGF, bFGF, MMP-2, MMP-7, and MMP-9 (Figs. 4, 5).

TS content and DPD activity

The results for TS and DPD are summarized in Fig. 6a, b. For DPD assays, DPD activity had a tendency to decrease in the treatment group, particularly IFN-α and S-1 group. For the TS assay, a large variation was not observed.

Comparison of gene profiles of implanted tumors using cDNA microarray

In Figs. 4 and 5, we investigated six representative angiogenic factors. The six angiogenic factors significantly decreased. Then, a comparison of 124 (52 genes involved in response to the 5-FU and other anticancer drugs, and 72 genes involved in metastasis and invasion) gene expressions on subcutaneously implanted tumors was conducted using a cDNA microarray. In addition to VEGF, bFGF, CD31, MMP-2, MMP-7, and MMP-9, we detected the 1 upregulated gene: SERPINE1, and 6 downregulated genes: SERPINB2, VEGFC, TGFb2, FLT1, MMP16, and ITGB3, defined in a range of twofold difference (Table 4).

Discussion

In the present study, we assessed the effect of the combination of IFN-α and S-1 administration on pancreatic carcinoma. To our knowledge, this is the first report to show that human IFN-α combined with S-1 administration significantly inhibited the growth of human pancreatic cancer.

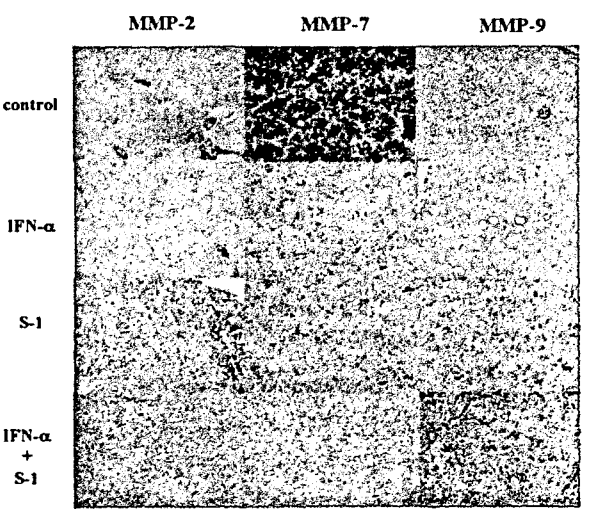

Fig. 5 Effects of IFN-α and S-1 detected by immunohistochemical analysis. Tumors were harvested from control mice and mice treated with IFN-α, S-1, or both. The sections were immunostained for expression MMP-2, MMP-7, and MMP-9. Tumors from mice treated with IFN-α and S-1 had a decrease in MMP-2, MMP-7, and MMP-9. *Representative samples* (× 200) are shown

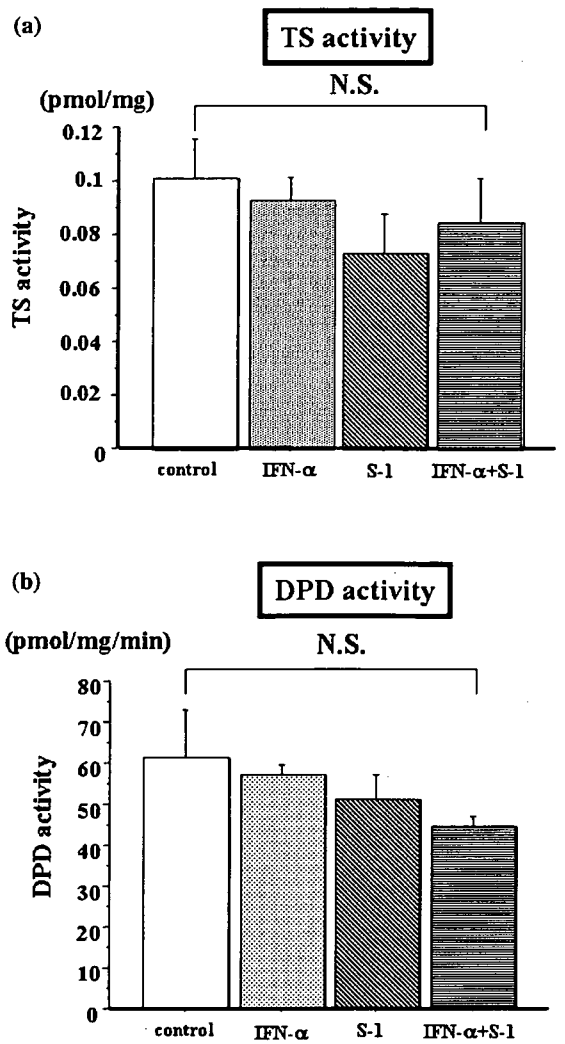

Fig. 6 **a, b** Thymidylate synthase and DPD activity of pancreatic cancer xenografts. The TS activity was determined on the method described by Spears et al. [29]. The DPD activity was measured according to the procedures of Takechi et al. [31]. The *error bars* indicate the standard deviation

The majority of advanced pancreatic cancer is drug-resistant. Despite advances in recent chemotherapy, the subject about drug resistance is not resolved. Recently, combination chemotherapy of IFN-α with 5-FU, and other agents was to some extent useful to suppress growth of various cancers [20, 32, 33], because IFN-α is biochemical modulator of 5-FU and also has antineoplastic effect. However, the mechanism of effectiveness combination therapy is unclear. Previous studies showed that IFN-α reduced 5-FU clearance and altered 5-FU metabolism (i.e., increased the quantity of 5-fluoro-dUMP that can bind to thymidylate synthetase), resulting in inhibition of conversion of

Table 4 cDNA microarray (control vs. IFN-α and S-1)

Gene name	Abbreviated name	Genbank accession number	FC[a]
Upregulated gene			
SERPINE1	PAI-1	NM_000602	2.11
Downregulated gene			
SERPINB2	PAI-2	NM_002575	0.10
VEGFC	VEGFC	NM_005429	0.33
TGFb2	TGFβ2	NM_003238	0.34
FLT1	Flt-1	NM_002019	0.41
MMP16	MT3	NM_022564	0.42
ITGB3	β3	NM_000212	0.48

PAI-1 Plasminogen activator inhibitor-1; *PAI-2* Serine (or cysteine) proteinase inhibitor, clade B (ovalbumin), member 2; *VEGFC* Vascular endothelial growth factor C preproprotein; *TGF(2* Transforming growth factor, beta 2; *Flt-1* Fms-related tyrosine kinase 1 (vascular endothelial growth factor/vascular permeability factor receptor); *MT3* Matrix metalloproteinase 16 isoform 2; *β3* Integrin beta chain, beta 3 precursor

[a] Fold change

dUMP to dTMP during normal DNA synthesis [34, 35]. It seems that IFN-α reduces the uptake of thymidine and the activity of thymidine kinase in conjunction with the action of 5-FU. Changes in the 5-FU metabolic pathway could be one of the underlying mechanisms of IFN-α synergism. In this context, it is of note that Kaneko et al. [32] recently reported that the thymidylate synthetase inhibition rate was increased and the quantity of 5-fluoro-dUMP was decreased following treatment with IFN-α and 5-FU.

A new oral antineoplastic agent, S-1, is based on biochemical modulation of 5-FU. In short, it is designed to enhance anticancer activity and reduce gastrointestinal toxicity through the deliberate combination of the following components: an oral fluoropyrimidine agent, tegafur (FT), which is a masked form of 5-FU, a DPD inhibitor CDHP (5-chloro-2, 4-dihydroxypyridine), which is an inhibitor of 5-FU degradation and an ORTC (orotate phosphoribosyltransferase) inhibitor, Oxo (potassium oxonate), which is an inhibitor of 5-FU phosphorylation, which is localized in the gastrointestinal tract. S-1 was devised as a combination drug with a molar ratio of 1:0.4: 1 for FT, CDHP, and Oxo, respectively. Briefly, S-1 has cytotoxic mechanisms similar to those of 5-FU, but has been shown to have less-toxic side-effects than 5-FU in clinical trials [36]. Moreover, S-1 has been shown to have antitumor activity far superior to 5-FU against human tumor xenografts [37].

Recent clinical study has shown that DPD activity in pancreatic cancer is much higher than in various other solid tumors. In the present study, DPD activity has a tendency to decrease in the combination of IFN-α and S-1 group.

In cell proliferation assay, the growth of cancer was inhibited significantly with IFN-α and S-1 ($P < 0.001$). In the analysis of tumor growth, treatment with daily IFN-α alone or S-1 alone reduced the growth of primary neoplasms only by 3 and 16%, respectively. The combination therapy with IFN-α and S-1 further decreased tumor growth by 74%. Daily doses of IFN-α and S-1 were well tolerated by nude mice. IHC analyses of the pancreatic cancers demonstrated a significant decrease in $PCNA^+$ cells, an associated increase in $TUNEL^+$ cells, and a significant decrease in MVD in the IFN-α treated or IFN-α and S-1-treated tumors. The reduction in MVD was due to a significant increase in endothelial cell apoptosis. The reduction in MVD is noteworthy because the progressive growth and metastasis of malignant neoplasms depend on adequate neovascularization. The balance between the proangiogenic and antiangiogenic molecules released by tumor cells and surrounding host cells determines the extent of angiogenesis. Among the major proangiogenic molecules, IFN-α has been shown to inhibit protein production of bFGF, MMP-9, IL-8, and VEGF [38].

In the present study, administration of human IFN-α and S-1 six times a week decreased the expression of VEGF, bFGF, MMP-2, MMP-7, and MMP-9 in human pancreatic cancer cells. These are important survival factors for human and mouse endothelial cells, and this decreased expression correlated with an increased apoptosis of endothelial cells. The combination therapy with IFN-α and S-1 enhanced apoptosis of endothelial cells and clearly decreased MVD, i.e., vascularization, leading to apoptosis of tumor cells and the surrounding stroma.

The median survival in combination treatment group was not improved compared with other treatment groups, but the median survival in the treated groups was longer compared with the control group (control vs. IFN-α, S-1 (8 mg/kg), IFN-α and S-1 (8 mg/kg), $P < 0.05$). Actually, this is consistent with the previous report that there is no difference between the combination and the treatment with 5-FU or interferon in clinic [39] which may be caused by unknown mechanism in the combination group.

Our microarray data provided information on seven genes differentially expressed in IFN-α and S-1 group. The upregulated gene was *SERPINE1*, which encodes plasminogen activator inhibitor-1 (PAI-1). The PAI-1 belongs to the family of serine protease inhibitors. It is implicated in processes such as tissue remodeling, thrombolysis, tumor invasion, and metastasis. Clinical investigations show a strong and independent prognostic value of PAI-1 in primary pancreatic cancer. The downregulated genes included *SERPINB2, VEGFC, TGFb2, FLT1, MMP16, ITGB3*, which encode PAI-2, VEGF-C, TGFβ2, Flt-1, MT3, β3. The PAI-2, a gene whose expression is linked to cell invasion, has been identified in head and neck tumor cell line. In addition, immunohistochemical evaluation of biopsy samples reveals a high expression of PAI-2 in both normal and dysplastic epithelia with a marked decrease of expression in areas of the biopsies containing HNSCC. It is reported that PAI-2 promotes extracellular matrix production and local invasion of pancreatic cancer. Vascular endothelial growth factor-C (VEGF-C) is the first lymphangiogenic factor identified. Moreover, there is ample evidence for the expression of VEGF-C in human tumors. Furudoi et al. [40] suggested that the expression of VEGF-C was correlated with lymphatic and venous invasion, lymph node status, and microvessel density. In pancreatic cancer, lymphatic invasion and the development of metastases are also associated with VEGF-C expression. Transforming growth factor-beta2 (TGF-β2) is a member of the TGF-β family. The $TGF\text{-}\beta2^{+/-}$ mice are viable but exhibit hyperplasia of Cowper's gland duct. With the full loss of TGF-β2 ($TGF\text{-}\beta2^{-/-}$), mice die at birth with defects in their lungs, heart, spinal column, and various other organs. Furthermore, the TGF-β2 may serve as an interim regulator of the MUC4 expression, morphology, and metastasis of human pancreatic cancer regulated by a local host microenvironment. Fms-related tyrosine kinase 1 (Flt-1) is a transmembrane receptor protein for vascular endothelial growth factor/vascular permeability factor receptor. The Flt-1 is involved in positive regulation of cell proliferation, pregnancy, protein amino acid phosphorylation, and angiogenesis. On pancreatic cancer, it is reported that the Flt-1may promote migration and invasion. Membrane-tethered MMP-16/MT3-MMP is the member of the membrane type MMP subfamily which, in addition to MT3-MMP, includes MT1-MMP, MT2-MMP, MT4-MMP, MT5-MMP, and MT6-MMP. The overexpression of MMP-16/MT3-MMPs reduces integrin-mediated cell adhesion without changing the cell surface expression and assembly of integrin subunits. The β3 is the subunit of integrin αIIbβ, including integrin-mediated signaling pathway, blood coagulation, cell-matrix adhesion, and development. Little is known about the MMP-16 and integrin in human pancreatic cancer.

Among these genes, VEGFC, FLT1, β3 are important genes in the processes of tumor invasion and metastasis. It appeared that these downregulated genes caused the growth inhibition of xenografted tumor in the present study.

In summary, we show that the combination therapy of IFN-α and S-1 significantly reduces the growth of human pancreatic carcinoma in nude mice. The combination therapy of IFN-α and S-1 decrease $PCNA^+$ positive cells and increase $TUNEL^+$ cells. Moreover, antiangiogenic factors are also inhibited, respectively. Therefore, this combination therapy may provide a new approach to the treatment of a devastating disease.

Acknowledgments This study was supported by a part of The Board for Cancer Research Project Cooperated by TAIHO Pharmaceutical Co., Ltd and The University of Tokushima.

References

1. Parker SL, Tong T, Bolden S, Wingo PA (1997) Cancer statistics. CA Cancer J Clin 47:5–27
2. Yeo CJ, Cameron JL (1999) Pancreatic cancer. Curr Probl Surg 36:59–152
3. Isaacs A, Lindenmann J (1957) Virus interference I. The interferon. Proc R Soc Lond 147:258–267
4. Baron S, Dianzani F (1994) The interferons: a biological system with therapeutic potential in viral infections. Antiviral Res 24:97–110
5. Hertzog PJ, Hwang SY, Kola I (1994) Role of interferons in the regulation of cell proliferation, differentiation and development. Mol Reprod Dev 39:226–232
6. Gutterman JU (1994) Cytokine therapeutics: lessons from interferon-α. Proc Natl Acad Sci USA 91:1198–1205
7. Krown SE (1988) Interferons in malignancy: biological products or biological response modifiers? J Natl Cancer Inst (Bethesda) 80:306–309
8. Singh RK, Bucana CD, Gutman M, Fan D, Wilson MR, Fidler IJ (1994) Organ-site dependent expression of bFGF in human renal cell carcinoma cells. Am J Pathol 145:365–374
9. Oliveira IC, Sciavolino PJ, Lee TH, Vilcek J (1992) Downregulation of interleukin-8 gene expression in human fibroblasts: unique mechanism of transcriptional inhibition of interferon. Proc Natl Acad Sci USA 89:9049–9053
10. Fabra A, Nakajima M, Bucana CD, Fidler IJ (1992) Modulation of the invasive phenotype of human colon carcinoma cells by fibroblasts from orthotopic or ectopic organs of nude mice. Differentiation 52:101–110
11. Schiller JH, Storer B, Bittner G, Willson JK, Borden EC (1988) Phase II trial of a combination of interferon-β ser and interferon-γ in patients with advanced malignant melanoma. J Interferon Res 8:581–589
12. Shirasaka T, Nakano K, Fukushima M, Takechi T, Satake H, Uchida J, Fujioka A, Saito H, Okabe H, Oyama K, Takeda S, Unemi N, Fukushima M (1996) Antitumor activity of 1 M-tegaful- 0.4 M 5-chloro-2, 4-dihydroxypyridine-1M potassium oxonate (S-1) against human colon carcinoma orthotopically implanted into nude rats. Cancer Res 56:2602–2606
13. Au JL, Sadee W (1980) Activation of Ftorafur [R,S-1-(tetrahydro-2-furanyl)-5-fluorouracil] to 5-fluorouracil and gamma-butyrolactone. Cancer Res 40:2814–2819
14. Tatsumi K, Fukushima M, Shirasaka T, Fujii S (1987) Inhibitory effects of pyrimidine, barbituric acid and pyridine derivatives on 5-fluorouracil degradation in rat liver extracts. Jpn J Cancer Res 78:748–755
15. Shirasaka T, Shimamoto Y, Fukushima M (1993) Inhibition by oxonic acid of gastrointestinal toxicity of 5-fluorouracil without loss of its antitumor activity in rats. Cancer Res 53:4004–4009
16. Sakata Y, Ohtsu A, Horikoshi N, Sugimachi K, Mitachi Y, Taguchi T (1998) Late phase II study of novel oral fluoropyrimidine anticancer drug S-1 (1 M tegafur-0.4 M gimestat-1 M otastat potassium) in advanced gastric cancer patients. Eur J Cancer 34:1715–1720
17. Ohtsu A, Baba H, Sakata Y, Mitachi Y, Horikoshi N, Sugimachi K, Taguchi T (2000) Phase II study of S-1, a novel oral fluoropyrimidine derivative, in patients with metastatic colorectal carcinoma. Br J Cancer 83:141–145
18. Hayashi K, Imaizumi T, Uchida K, Kuromachi H, Takasaki K (2002) High response rates in patients with pancreatic cancer using the novel oral fluoropyrimidine S-1. Oncol Rep 9:1355–1361
19. Wadler S, Schwartz EL, Goldman M, Lyver A, Itri L, Wiernik PH (1988) Preclinical and clinical studies of 5-fluorouracil (FURA) and recombinant α-2a-interferon (IFN) against gastrointestinal (GI) malignancies. Clin Res 36:803A
20. Sakon M, Nagano H, Dono K, et al (2002) Combined intraarterial 5-fluorouracil and subcutaneous interferon-α therapy for advanced hepatocellular carcinoma with tumor thrombi in the major portal branches. Cancer 94:435–442
21. Schwartz EL, Hoffman M, O'Connor CJ, Wadler S (1992) Stimulation of 5-fluorouracil metabolic activation by interferon-α in human colon carcinoma cells. Biochem Biophys Res Commun 182:1232–1239
22. Elias L, Sandoval JM (1989) Interferon effects upon fluorouracil metabolism by HL-60 cells. Biochem Biophys Res Commun 163:867–874
23. Eguchi H, Nagano H, Yamamoto H et al (2000) Augmentation of antitumor activity of 5-fluorouracil by interferon-α is associated with up-regulation of p27Kip1 in human hepatocellular carcinoma cells. Clin Cancer Res 6:2881–2890
24. Bruns CJ, Harbison MT, Kuniyasu H, Eue I, Fidler IJ (1999) In vivo selection and characterization of metastatic variants from human pancreatic adenocarcinoma by using orthotopic implantation in nude mice. Neoplasia 1:50–62
25. Tominaga H, Ishiyama M, Ohseto F (1999) A water-soluble tetrazolium salt useful for colorimetric cell viability assay. Anal Commun 36:47
26. Wen Y, Yan DH, Wang B, Spohn B, Ding Y, Shao R, Zou Y, Xie K, Hung MC (2001) p202, an interferon-inducible protein, mediates multiple antitumor activities in human pancreatic cancer xenograft models. Cancer Res 61:7142–7147
27. Vecchi A, Garlanda C, Lampugnani MG, Resnati M, Matteucci C, Stoppacciaro A, Schnurch H, Risau W, Ruco L, Mantovani A (1994) Monoclonal antibodies specific for endothelial cells of mouse blood vessels: their application in the identification of adult and embryonic endothelium. Eur J Cell Biol 63:247–254
28. Weidner N, Semple JP, Welch WR, Folkman J (1991) Tumor angiogenesis and metastasis: correlation in invasive breast carcinoma. N Engl J Med 324:1–8
29. Spears CP, Shahinian AH, Moran RG, Heidelberger C, Corbett TH (1982) In vivo kinetics of thymidylate synthetase inhibition of 5-fluorouracil-sensitive and -resistant murine colon adenocarcinomas. Cancer Res 42:450–456
30. Terashima M, Irinoda T, Fujiwara H (2002) Roles of thymidylate synthase and dihydropyrimidine dehydrogenase on tumour progression and sensitivity to 5-fluorouracil in human gastric cancer. Anticancer Res 22:761–768
31. Takechi K, Tamura H, Yamaoka K, Sakurai H (1997) Pharmacokinetic analysis of free radicals by in vivo BCM (blood circulation monitoring)-ESR method. Free Radic Res 26:483–496

32. Kaneko S, Urabe T, Kobayashi K (2002) Combination chemotherapy for advanced hepatocellular carcinoma complicated by major portal vein thrombosis. Oncology 62:69–73
33. Picozzi VJ, Kozarek RA, Traverso LW (2003) Interferon-based adjuvant chemoradiation therapy after pancreaticoduodenectomy for pancreatic adenocarcinoma. Am J Surg 185:4767–4780
34. Schwartz EL, Hoffman M, O'Connor CJ, Wadler S (1992) Stimulation of 5-fluorouracil metabolic activation by interferon-α in human colon carcinoma cells. Biochem Biophys Res Commun 182:1232–1239
35. Elias L, Sandoval JM (1989) Interferon effects upon fluorouracil metabolism by HL-60 cells. Biochem Biophys Res Commun 163:867–874
36. Shirasaka T, Shimamato Y, Ohshimo H, Yamaguchi M, Kato T, Yonekura K, Fukushima M (1996) Development of a novel form of an oral 5-fluorouracil derivative (S-1) directed to the potentiation of the tumor selective cytotoxicity of 5-fluorouracil by two biochemical modulators. Anticancer Drugs 7:548–557
37. Fukushima M, Satake H, Uchida J, Shimamoto Y, Kato T, Okabe H (1998) Preclinical antitumor efficacy of S-1: a new oral formulation of 5-fluorouracil on human tumor xenografts. Int J Oncol 13:693–698
38. Fidler IJ, Ellis LM (1994) The implications of angiogenesis for the biology and therapy of cancer metastasis. Cell 79:185–188
39. Wagener DJ, Wils JA, Kok TC, Planting A, Couvreur ML, Baron B (2002) Results of a randomised phase II study of cisplatin plus 5-fluorouracil versus cisplatin plus 5-fluorouracil with alpha-interferon in metastatic pancreatic cancer: an EORTC gastrointestinal tract cancer group trial. Eur J Cancer 38:648–653
40. Furudoi A, Tanaka S, Haruma K, Kitadai Y, Yoshihara M, Chayama K, Shimamoto F (2002) Clinical significance of vascular endothelial growth factor C expression and angiogenesis at the deepest invasive site of advanced colorectal carcinoma. Oncology 62:157–166

Int J Clin Oncol (2007) 12:111–119
DOI 10.1007/s10147-006-0634-x

ORIGINAL ARTICLE

Kotaro Miyake · Satoru Imura · Tomoharu Yoshizumi
Tetsuya Ikemoto · Yuji Morine · Mitsuo Shimada

Role of thymidine phosphorylase and orotate phosphoribosyltransferase mRNA expression and its ratio to dihydropyrimidine dehydrogenase in the prognosis and clinicopathological features of patients with pancreatic cancer

Received: July 3, 2006 / Accepted: October 31, 2006

Abstract
Background. Thymidine phosphorylase (TP), orotate phosphoribosyltransferase (OPRT), and dihydropyrimidine dehydrogenase (DPD) are important enzymes related to the metabolism of 5-fluorouracil and its derivatives. In this study, we analyzed the expression of these enzymes and evaluated the association between the expression of these enzymes and clinicopathological features and prognosis in patients with pancreatic cancer.
Methods. TP, OPRT, and DPD mRNA expressions were detected using a real-time reverse transcriptional-polymerase chain reaction method or by immunohistochemistry, using surgical specimens obtained from 25 patients with pancreatic cancer.
Results. TP mRNA expression was lower in cases with an alpha infiltration growth pattern than in cases with other infiltration growth patterns ($P < 0.05$). OPRT mRNA expression was higher in poorly differentiated-type cases than in differentiated type cases ($P < 0.05$). TP-, OPRT-, and DPD-positive stainings were found in 15 of 24 cases (63%), 10 of 19 cases (53%), and 14 of 21 cases (67%), respectively. There were significant correlations or trends between the mRNA and protein expressions of TP, OPRT, and DPD. Patients with a low TP/DPD ratio survived significantly longer than those with a high ratio ($P < 0.05$). Multivariate analysis demonstrated a significantly poorer outcome in patients with a high TP/DPD ratio compared with in patients with a low ratio ($P < 0.05$).
Conclusion. The TP/DPD ratio might be useful as a prognostic factor in patients with pancreatic cancer.

K. Miyake · S. Imura · T. Yoshizumi · T. Ikemoto · Y. Morine · M. Shimada (✉)
Department of Digestive and Pediatric Surgery, Institute of Health Biosciences, The University of Tokushima Graduate School, 3-18-15 Kuramoto, Tokushima 770-8503, Japan
Tel. +81-88-633-9276, 9277; Fax +81-88-631-9698
e-mail: mshimada@clin.med.tokushima-u.ac.jp

Key words Pancreatic cancer · Thymidine phosphorylase · Orotate phosphoribosyltransferase · Laser-capture microdissection

Introduction

One of the most widely used antitumor chemotherapeutic agents for the treatment of a variety of gastrointestinal cancers is 5-fluorouracil (5-FU). 5-FU is catabolized to dihydrofluorouracil by the first- and rate-limiting enzyme, dihydropyrimidine dehydrogenase (DPD).[1] By itself, 5-FU is inactive, and it requires intracellular conversion to 5-fluoro-2′-deoxyuridine 5′-monophosphate (FdUMP) by thymidine phosphorylase (TP), orotate phosphoribosyltransferase (OPRT), uridine phosphorylase (UP), and thymidine kinase (TK). 5-FU exerts its cytotoxic activity through the formation of a ternary complex with thymidylate synthase (TS) and 5,10-methylene-tetrahydrofolate, resulting in inhibition of TS and blockade of the DNA synthetic process.[2,3]

TP is the enzyme that regulates intracellular pyrimidine metabolism via the degradation of thymidine to thymine and it is highly expressed in the normal liver and intestine, and in various human cancer cells. TP has been recognized as a prognostic factor because it is the same protein as platelet-derived endothelial cell growth factor (PD-ECGF).[4–8] It is a key enzyme in the conversion of 5′-deoxy-5-fluorouridine (5′-DFUR), a prodrug of 5-FU, and capecitabine, a prodrug of 5′-DFUR, to 5-FU.[9,10] OPRT is the first-limiting enzyme in this 5-FU conversion, leading to the formation of FdUMP in the presence of 5-phosphoribosyl-1-pyrophosphate as a cofactor.[11,12] Previous studies have demonstrated that adenovirus-mediated transduction of the *OPRT* gene resulted in a marked sensitization to 5-FU cytotoxicity in the cells of colon, gastric, hepatic, and pancreatic cancers.[13,14] Thus, OPRT is an important enzyme in 5-FU activation. In addition, OPRT, which converts orotic acid to orotidine 5′-phosphate, is the rate-limiting enzyme in the de novo process of DNA and RNA synthesis. DPD is the first- and rate-limiting en-

zyme for the catabolism of 5-FU.[1] High DPD mRNA levels have been shown in various human cancers and cell lines with low sensitivity to 5-FU.[15–17]

Recently, it was revealed that the efficacy of 5′-DFUR was correlated with the ratio of TP to DPD (TP/DPD ratio) activity in human cancer xenograft models.[18] A clinical study using 5′-DFUR showed that patients with a high TP/DPD ratio in gastric cancer tissues had longer disease-free survival than patients with a low TP/DPD ratio.[19] Furthermore, both OPRT mRNA expression and the OPRT/DPD ratio might be useful as predictive parameters for the efficacy of fluoropyrimidine-based chemotherapy for metastatic colorectal cancer.[20]

Although TP, OPRT, and DPD are important enzymes involved in 5-FU cytotoxicity and DNA synthesis, to our knowledge, this is the first report about TP, OPRT, and DPD mRNA expressions in pancreatic cancer. In the present study, we investigated the relationship between TP, OPRT, and DPD expressions and clinicopathological features and survival in patients with pancreatic cancer.

Patients and methods

Patient characteristics

A total of 39 pancreatic cancer patients who underwent surgical treatment between March 1994 and March 2004 at Tokushima University Hospital were enrolled in this study. Among these patients, 14 patients were excluded because the condition of the formalin-fixed, paraffin-embedded tumor specimen was not adequate. Thus, TP, OPRT, and DPD mRNA were detected, using a real-time reverse transcriptional-polymerase chain reaction (RT-PCR) method, from the tumor specimens of only 25 patients with pancreatic cancer.

Of the 25 patients, 16 were men and 9 women, with a mean age of 62.9 years, ranging from 36 to 79 years. None had received prior chemotherapy or irradiation before the surgery. Three patients did not receive any chemotherapy after surgery, 16 patients received 5-FU or tegafur uracil, and 7 patients received gemcitabine, as adjuvant chemotherapy.

Patient characteristics and several clinicopathological features (age, sex, tumor size, histological type, infiltration growth pattern, lymphatic invasion, venous invasion, local advance, lymph node metastasis, distant metastasis, and stage) were examined according to the criteria of the *Classification of pancreatic carcinoma*, second English edition.[21] This study was authorized in advance by the institutional review board of the University of Tokushima Graduate School, and all patients provided written informed consent.

Microdissection in primary tumors

A representative formalin-fixed, paraffin-embedded tumor specimen, which contained a central section of the cancer, was selected from each of the lesions by a pathologist after an examination of the hematoxylin-and-eosin-stained slides. Then 10-μm-thick sections were stained with nuclear fast red to enable visualization of histology, and laser-capture microdissection (PALM Microlaser Technologies, Munich, Germany) was performed to ensure the presence of malignant cells in the microcentrifuge tube.

RNA extraction and cDNA synthesis from paraffin-embedded tissues

RNA for each sample was extracted according to a previously described method, with minor modifications.[16,17,19] Briefly, 600 μl of xylene was added to each tube. After centrifugation for 7 min at 20800 *g*, the supernatant was discarded, and the washing step was repeated three times. The deparaffinized materials were rehydrated in xylene/ethanol/water. The rehydration medium was removed after centrifugation for 7 min at 20800 *g*. After discarding the last supernatant, the pelleted sections were resolved in 70% ethanol. Then 400 μl of buffer (4 M guanidine isothiocyanate solution including 0.5% sarcosine and 8 μl 1 M dithiothreitol [DTT]) were added to the dried tissue and homogenized mechanically. For RNA demodification, homogenates were heated at 95°C for 30 min. RNA was extracted from homogenates by the addition of 50 μl of 2 M sodium acetate (pH 4.0), 500 μl of water-saturated phenol, and 100 μl of chloroform-isoamyl mixture (49:1). RNA was recovered from the water phase by isopropanol precipitation and transferred to a new tube and precipitated with 10 μl glycogen and 400 μl isopropanol for 30 min at −20°C. After centrifugation for 7 min at 20800 *g*, the pellet was washed with 500 μl 75% ethanol. After drying, the pellet was dissolved in 50 μl 5 mM Tris HCl (pH 8.0). Reverse transcription was carried out at 39°C for 45 min, using 400 units of Moloney murine leukemia virus (MMLV) reverse transcriptase, 1 × first-strand buffer, 0.04 μg/μl random hexamers, 10 mM DTT, and 1 mM deoxynucleoside triphosphate.

PCR quantification of mRNA expression

Target cDNA sequences were amplified by quantitative PCR, using a fluorescence-based real-time detection method (ABI Prism 7900 Sequence Detection System, TaqMan; Applied Biosystems, Foster City, CA, USA) as previously described[22]. PCR was carried out for each gene of interest and β-actin was used as an internal reference gene. The 25-μL PCR reaction mixture contained 600 nmol/l of each primer; 200 nmol/l each of dATP, dCTP, and dGTP; 400 μmol/l dUTP; 5.5 mmol/l $MgCl_2$; and 1 × TaqMan buffer containing a reference dye. The primers and probe sequences used were as follows: TP primers, CCTGCGGACG GAATCCT and GCTGTGATGAGTGGCAGGCT, probe 6FAM (carboxyfluorescein)-5′-CAGCCAGAGATGTGA CAGCCACCGT-3′TAMRA (N,N,N0,N0-tetramethyl-6-carboxyrhodamine);[20] OPRT primers, TCCTGGGCAGAT CTAGTAAATGC and TGCTCCTCAGCCATTCTA ACC, probe 6FAM-5′-CTCCTTATTGCGGAAATGAG CTCCACC-3′TAMRA;[20] DPD primers, AGGACGCAA GGAGGGTTTG and GTCCGCCGAGTCCTTACTGA,

probe 6FAM-5′-CAGTGCCTACAGTCTCGAGTCTGC CAGTG3′TAMRA;[23] β-actin primers, TGAGCGCGGC TACAGCTT and TCCTTAATGTCACGCACGATTT, β-actin probe 6FAM-5′-ACCACCACGGCCGAGCGG-3′TAMRA. The PCR conditions were 50°C for 10s and 95°C for 10min, followed by 42 cycles at 95°C for 15s and 60°C for 1min. Relative gene expressions of *TP* and *OPRT* were determined based on the threshold cycles of each gene in relation to the threshold cycle of the corresponding internal standard β-actin.

The use of β-actin as a reference gene avoids the need for RNA concentration measurement. The β-actin real-time PCR analysis also estimated the amount of extracted mRNA. The rise of the β-actin signal after 37 cycles under the described conditions indicated an insufficient amount of mRNA present for the subsequent TP and OPRT quantitation. When measuring gene expressions in paraffin-embedded tissues, the median value of the threshold cycle of β-actin was 26 cycles, ranging from 23 to 28.

Immunohistochemical staining

Sections of 4-μm-thick paraffin-embedded tumor specimen were dewaxed and rehydrated with xylene and ethanol. After immersion in 10mM citrate buffer (pH 6.0), the slides underwent microwave pretreatment for 10min for optimal antigen retrieval. The sections were then incubated overnight at 4°C with rabbit polyclonal DPD and OPRT antibodies (1:200 for DPD dilution, and 1:500 for OPRT dilution; Taiho Pharmaceutical, Tokyo, Japan) and with mouse monoclonal TP antibody (1:100 dilution; Nippon Roche Research Center, Tokyo, Japan). The secondary antibody was biotin-labeled and was applied for 30min. A streptavidin-LSA amplification method (DAKO K0679, Dako Cytomation, Carpinteria, CA, USA) was carried out for 30min, followed by peroxidase/diaminobenzidine substrate/chromagen treatment. The slides were counterstained with hematoxylin.

Positive expressions of TP, OPRT, and DPD proteins were determined by counting the number of tumor cells with cytoplasmic staining. The cases with staining were classified into two groups according to the percentage of positively stained tumor cells in all fields: low expression (negative or positive in <30% of tumor cells) and high expression (positive in ≥30% of tumor cells).[24,25]

Statistical analysis

Statistical analysis was performed using StatView 5.0J software (SAS Institute, Cary, NC, USA). The Mann-Whitney *U*-test or the Kruskal-Wallis test was used to compare TP or OPRT – and its ratio to DPD mRNA expression – with the clinicopathological features. Survival analysis was done by the Kaplan-Meier method and survivals were compared by the log-rank test. Cox's proportional hazard regression model was used for a multivariate analysis. The χ^2 test was used for correlations between the mRNA and protein expressions of TP, OPRT, and DPD. A P value of less than 0.05 was taken as significant.

Results

TP, OPRT, and DPD mRNA expressions in pancreatic cancer

The correlations between clinicopathological features and the mRNA expressions of TP, OPRT, and DPD are shown in Table 1. The median values of TP, OPRT, and DPD mRNA expressions were 5.10 (range, 2.58–37.09), 0.83 (range, 0.46–1.77), and 0.98 (range, 0.62–4.13), respectively. TP mRNA expression was lower in cases with an alpha infiltration growth pattern than in cases with other patterns ($P < 0.05$). OPRT mRNA expression was higher in poorly differentiated cases than in differentiated cases ($P < 0.05$). DPD mRNA expression in pancreatic cancer showed no statistically significant differences in relation to any clinicopathological features.

Ratio of TP or OPRT to DPD in pancreatic cancer

The correlations between clinicopathological features and both the TP/DPD and OPRT/DPD ratios are shown in Table 2. The median values of the TP/DPD and OPRT/DPD ratios were 5.15 (range, 1.95–22.43) and 0.84 (range, 0.24–2.33), respectively. The TP/DPD and OPRT/DPD ratios showed no statistically significant correlation with any clinicopathological features.

Immunohistochemical study of TP, OPRT, and DPD expressions

TP protein expression was immunohistochemically seen in the cytoplasm and nuclei of cancer cells, whereas OPRT and DPD protein expressions were seen in the cytoplasm. As shown in Fig. 1, positive stainings for TP, OPRT, and DPD were found (in 15 of 24 cases [63%], 10 of 19 cases [53%], and 14 of 21 cases [67%], respectively).

Correlations between mRNA and protein expressions of TP, OPRT, and DPD

The median values of TP, OPRT, and DPD mRNA expressions were 5.10 (range, 2.58–37.09), 0.83 (range, 0.23–1.77) and 0.98 (range, 0.29–4.13), and these means were selected as cutoff values to separate high and low mRNA expression of TP, OPRT, and DPD. There were significant correlations between the mRNA and protein expressions of TP, OPRT, and DPD ($P = 0.015$, $P = 0.040$, and $P = 0.026$, respectively; Table 3).

Survival

The median survival time in the patients with high TP and OPRT mRNA expressions was not different from that in the patients with low TP and OPRT mRNA expressions. The median values of the TP/DPD and OPRT/DPD ratios in patients with high and low TP and OPRT mRNA expres-

Table 1. Correlation between clinicopathological features and TP, OPRT, and DPD mRNA expressions in pancreatic cancer

Variables	Number of patients ($n = 25$)	TP mRNA expression		OPRT mRNA expression		DPD mRNA expression	
		Median	*P* value	Median	*P* value	Median	*P* value
Age (years)	62 (36–79)						
Sex							
Male	16	4.56 (2.58–11.93)	0.456	1.00 (0.53–1.77)	0.353	0.94 (0.62–4.13)	0.168
Female	9	6.03 (3.79–37.09)		1.01 (0.46–1.25)		1.55 (0.86–1.94)	
Tumor size							
ts1,2	11	6.16 (2.58–9.43)	0.543	1.01 (0.67–1.64)	0.514	1.33 (0.86–4.13)	0.619
ts3,4	14	3.69 (3.06–37.09)		0.88 (0.46–1.77)		1.03 (0.62–1.94)	
Histological type							
Differentiated	22	5.51 (2.58–6.84)	0.760	0.83 (0.46–1.64)	0.046	1.10 (0.62–4.13)	0.547
Poorly differentiated	3	5.03 (3.59–37.09)		1.55 (1.33–1.77)		0.99 (0.76–1.34)	
Infiltration pattern							
Alpha	5	3.53 (2.58–11.93)	0.015	1.33 (0.55–1.77)	0.371	0.76 (0.62–1.34)	0.132
Beta and gamma	20	6.16 (3.06–37.09)		0.92 (0.46–1.64)		1.10 (0.73–4.13)	
Lymphatic invasion[a]							
ly0	8	4.23 (2.58–37.09)	0.602	1.13 (0.76–1.77)	0.233	0.98 (0.62–4.13)	0.349
ly1,2,3	14	6.08 (3.06–9.53)		0.83 (0.46–1.40)		1.10 (0.88–1.94)	
Venous invasion[a]							
v0	8	4.99 (2.58–9.43)	0.664	1.21 (0.55–1.40)	0.126	1.33 (0.62–4.13)	0.349
v1,2,3	14	5.57 (3.06–37.09)		0.83 (0.46–1.77)		0.97 (0.73–1.94)	
Local advance							
T2,3	13	6.03 (2.58–37.09)	0.931	0.83 (0.55–1.77)	0.680	1.02 (0.62–4.13)	0.670
T4	12	4.87 (3.06–11.93)		1.13 (0.46–1.25)		1.13 (0.86–1.94)	
Lymph node metastasis							
N0	9	5.10 (2.58–11.93)	0.801	1.01 (0.55–1.77)	0.390	0.99 (0.62–4.13)	0.396
N1,2,3	16	4.99 (3.06–37.09)		0.82 (0.46–1.64)		1.10 (0.73–1.94)	
Distant metastasis							
M0	22	7.60 (2.58–37.09)	0.695	0.83 (0.46–1.77)	0.184	0.99 (0.62–4.13)	0.338
M1	3	6.84 (3.06–11.93)		1.29 (1.24–1.33)		1.10 (1.34–1.58)	
Stage							
I,II,III	10	4.54 (2.58–37.09)	0.412	0.82 (0.55–1.77)	0.514	0.92 (0.62–4.13)	0.227
IV	15	6.03 (3.06–11.93)		1.99 (0.46–1.40)		1.23 (0.86–1.94)	

[a] In 3 patients, lymphatic and venous invasion are unclear

Table 2. Correlation between clinicopathological features and TP/DPD and OPRT/DPD ratios

Variables	Number of patients ($n = 25$)	TP/DPD ratio		OPRT/DPD ratio	
		Median	*P* value	Median	*P* value
Sex					
Male	16	5.34 (3.80–10.79)	0.127	0.91 (0.59–2.33)	0.063
Female	9	4.14 (1.95–22.43)		0.46 (0.24–1.46)	
Tumor size					
ts1,2	11	5.06 (2.28–6.68)	0.303	0.90 (0.25–1.68)	0.935
ts3,4	14	5.35 (1.95–22.43)		0.84 (0.24–2.33)	
Histological type					
Differentiated	22	5.08 (1.95–22.43)	0.934	0.79 (0.24–1.68)	0.111
Poorly differentiated	3	5.10 (4.95–5.13)		1.66 (0.99–2.33)	
Infiltration pattern					
Alpha	5	5.10 (4.95–5.78)	0.688	0.99 (0.89–2.33)	0.178
Beta and gamma	20	5.08 (1.95–22.43)		0.79 (0.24–1.68)	
Lymphatic invasion[a]					
ly0	8	5.10 (2.28–22.43)	0.640	0.99 (0.25–2.33)	0.193
ly1,2,3	14	4.82 (1.95–10.79)		0.73 (0.24–1.23)	
Venous invasion[a]					
v0	8	5.09 (2.28–9.57)	0.454	1.07 (0.25–2.33)	0.448
v1,2,3	14	5.10 (1.95–22.43)		0.79 (0.24–1.46)	
Local advance					
T2,3	13	5.10 (2.28–22.43)	0.522	0.90 (0.25–2.33)	0.680
T4	12	5.06 (1.95–10.79)		0.73 (0.24–1.46)	
Lymph node metastasis					
N0	9	5.13 (2.28–7.57)	0.316	0.90 (0.25–2.33)	0.618
N1,2,3	16	4.82 (1.95–22.43)		0.78 (0.24–1.68)	
Distant metastasis					
M0	22	5.06 (1.95–22.43)	0.281	0.89 (0.24–2.33)	0.791
M1	3	6.34 (5.10–7.57)		0.89(0.79–0.99)	
Stage					
I,II,III	10	5.09 (2.28–22.43)	0.722	0.90 (0.25–2.33)	0.744
IV	15	5.08 (1.95–10.79)		0.79 (0.24–1.46)	

[a] In 3 patients, lymphatic and venous invasiona are unclear

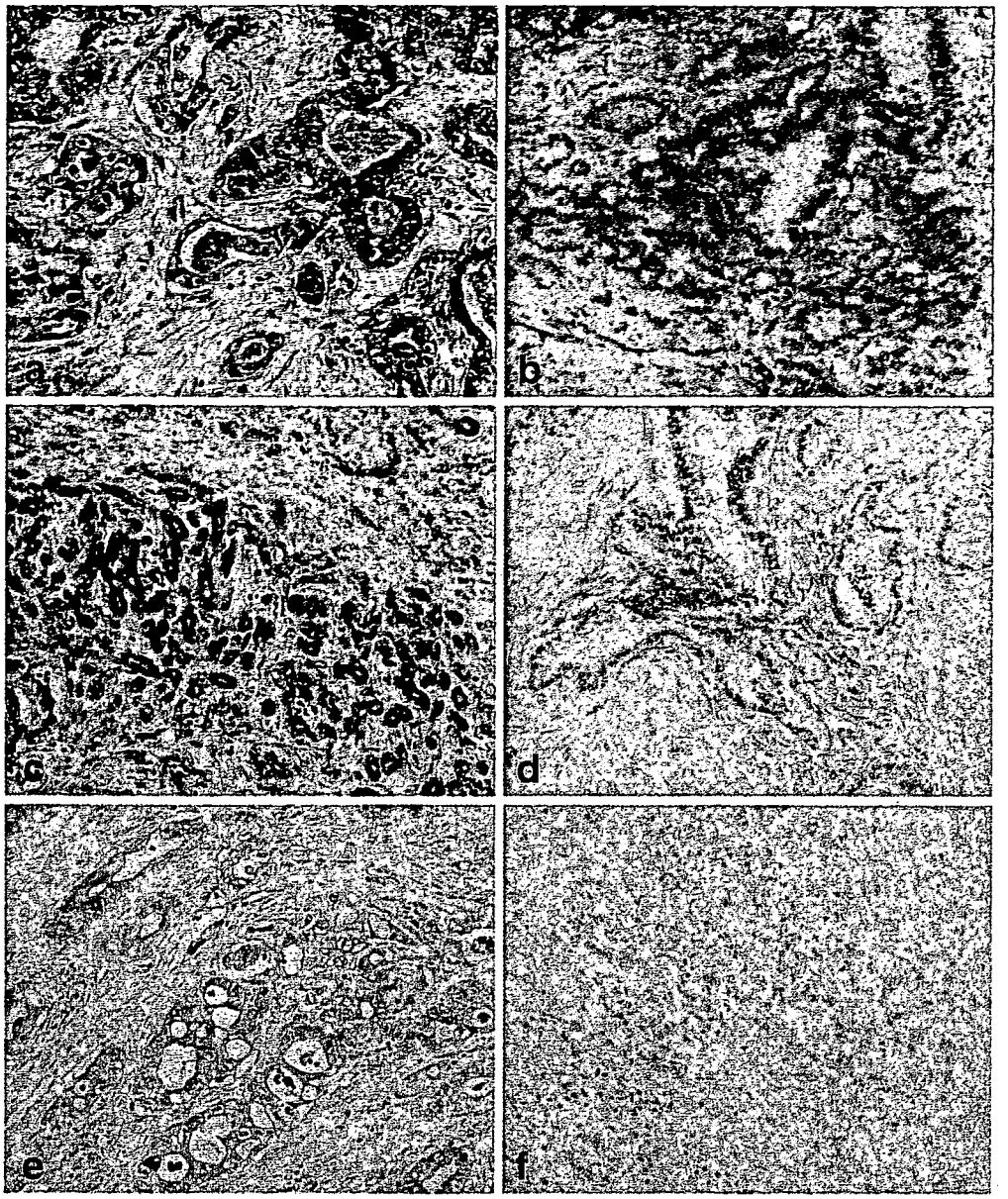

Fig. 1a–f. Representative photomicrographs of tissue sections immunostained for thymidine phosphorylase (TP), orotate phosphoribosyltransferase, (OPRT), and dihydropyrimidine dehydrogenase (DPD). **a** Pancreatic cancer with TP-positive expression. The signal was detected in the cytoplasm and nuclei of cancer cells. **b** Pancreatic cancer with TP-negative expression. **c** Pancreatic cancer with OPRT-positive expression. The signal was detected in the cytoplasm of cancer cells. **d** Pancreatic cancer with OPRT-negative expression. **e** Pancreatic cancer with DPD-positive expression. The signal was detected in the cytoplasm of cancer cells. **f** Pancreatic cancer with DPD-negative expression. **a–f** × 200

sions were 5.09 (range, 1.95–22.43) and 0.89 (range, 0.24–2.44), respectively, and these means were selected as cutoff values to separate high and low mRNA expression of TP/DPD and OPRT/DPD ratios.

As shown in Fig. 2, the log-rank test revealed that a higher TP/DPD ratio was associated with a poor outcome ($P = 0.02$), whereas the OPRT/DPD ratio was not so associated ($P = 0.23$; data not shown).

Factors related to patient prognosis were also evaluated using Cox proportional hazard univariate regression analysis. In addition to the established risk factors for pancreatic cancer (lymphatic invasion, local advance, and stage), the TP/DPD ratio was also related to survival. Factors considered to be univariately significant were additionally analyzed in a multivariate analysis. On multivariate analysis, only the TP/DPD ratio was found to be an independent prognostic factor (relative risk, 8.786; 95% confidence interval [CI], 1.593–48.470; $P < 0.005$; Table 4).

The correlation between TP, OPRT, and DPD and the chemotherapeutic outcome is shown in Table 5. There was no significant correlation between the chemotherapeutic regimen and survival.

Discussion

The correlation between the expressions of TS, DPD, TP, and OPRT and clinicopathological features in gastrointestinal cancer has already been reported by a large number of authors, based on biochemical assays, immunohistochemistry, enzyme-linked immunosorbent assay (ELISA), or PCR methods. In the present study, TP, OPRT, and DPD mRNA expressions in pancreatic cancer were measured by real-time RT-PCR combined with laser-capture microdissection. Our study showed that TP mRNA expression correlated